Entry

Physical Properties of Helium and Application in Respiratory Care

Eric Chappel [1,2]

1   Debiotech SA, Microsystems Department, 1004 Lausanne, Switzerland; e.chappel@debiotech.com or
     eric.chappel@hes-so.ch
2   HEPIA, HES-SO University of Applied Sciences and Arts Western Switzerland, 1202 Geneva, Switzerland

Definition: Helium is a low-density, inert, monoatomic gas that is widely used in medical applications. In respiratory care, Helium is mainly used as an adjunct therapy for patients with severe upper airway obstruction and asthma. To better understand the action mechanism of helium, the physical properties of several therapeutic gas mixtures with helium are calculated using kinetic theory. Flow in a simplified lung airways model is also shown to support the discussion of helium's respiratory benefits, including reduced work of breathing.

Keywords: helium; physical properties; kinetic theory; medical gases; airway resistance; work of breathing; respiratory care

1. Introduction

Helium is a noble gas that is used in a variety of applications. As the coldest liquefied gas, liquid helium makes it ideally suited in cryogenics, notably in the cooling of superconducting magnets in MRI (magnetic resonance imaging) scanners and NMR (nuclear magnetic resonance) spectrometers [1]. In gaseous form, helium has several industrial applications as a shielding gas during welding [2], a purge and pressurization gas [3], in leak detection [4], as a non-reactive carrier gas used in chromatography [5], and in semiconductor and optical fiber production [6]. Helium is also well known for its use as a lifting gas in balloons and blimps or in components of deep-diving breathing mixtures. As early as 1926, Sayers and Yant pointed out that the low solubility of helium compared to nitrogen could reduce the formation of gas bubbles and therefore decompression accidents among deep-sea divers [7]. In the medicine practice [8], helium is used in microscopy [9], radiology [10], and surgery [11], and it also has other promising applications in cardiology [12] and neurology [13]. However, the subject that has attracted a great deal of interest relates to the physiological benefits of breathing a mixture of helium and oxygen in patients suffering from severe upper airway obstruction and asthma. Helium was indeed considered a therapeutic gas from the 1930s due to its inert nature and its lightness compared to oxygen and nitrogen [14]. The respiratory care applications of helium capitalize on the unique properties of helium, which are examined in detail in this paper in relation to respiratory mechanics, and particular attention is paid to the several misconceptions about its viscosity and hypothetical hypothermic properties. A simple lung airways model based on pipe flow equations is also used to review the benefits of using helium mixtures as a function of the Reynolds number.

2. Physical Properties of Helium and Other Therapeutic Gas Mixtures

2.1. Origin, Discovery, and Extraction of Helium

Helium is the second most abundant element in the universe after hydrogen. These two elements represent 25% and 73% of its total mass, respectively [15,16], with all other elements constituting less than 2%. Most of the helium atoms in the universe were mainly created just a few minutes after the Big Bang through the Big Bang nucleosynthesis process [17,18]. Helium is also produced in stars by the fusion of hydrogen via the proton–

proton (p-p) chain reaction and the CNO cycle [19]. On earth, helium mainly results from the radioactive decay of uranium and thorium in the crust and the mantle of the earth, wherein alpha particles, i.e., He nuclei, $^4He^{2+}$, are emitted [20]. The balance between the degassing of He and its escape from the atmosphere by several processes leads to its atmospheric concentration being as low as 5.2 ppm by volume [21]. This noble gas is also very rare on Earth due to its inert nature, which prevents it from forming bonds with other atoms and therefore from being stored in the crust of the earth. Helium was discovered in 1868 by several observers who turned their spectroscopes on sun prominences during a total eclipse in the Indian Peninsula. The terrestrial equivalent of this unknown yellow spectral line was not observed until 1895 by Ramsay [22]. A few years later, the presence of helium was discovered in natural gas wells in Kansas, but its production really took off in the 1920s in order to produce enough helium for flying airships [23]. Today, helium is exclusively collected as a by-product of natural gas extraction and remains extremely rare. Only a limited number of countries produce it, with the United States and Russia being the main suppliers. The shortage of helium has become a growing concern in recent years, and the increase in demand coupled with the reduction in reserves has had a strong impact on its cost, which has doubled in recent years [24]. This trend will have to be considered in the development of medical devices, reinforcing the need to recycle gases in order to remain compatible with reimbursement policies.

2.2. Density

Helium is a colorless and odorless monoatomic gas that belongs to the noble gas family. Chemically inert and non-toxic, helium is generally considered by clinicians as medically inert, with no anesthetic effect, unlike nitrous oxide (N_2O) and xenon (Xe). Its atomic number is 2, and the atomic weight of its main abundant isotope, ^4He, is 4 g/mol (its nucleus contains 2 protons and 2 neutrons). The density of pure gas and gas mixtures can be easily estimated from the ideal gas law:

$$\rho = \sum_i x_i M_i \times \frac{P}{RT} \tag{1}$$

where ρ is the density in g/m^3, P is the absolute pressure in Pa, $R = 8.314$ J/(mol.K) and is the ideal gas constant, T is the temperature in Kelvin, x_i is the molar fraction of the pure gas component, and M_i is the molecular weight in g/mol of the pure gas component. Table 1 shows the density of several pure gases and gas mixtures that are used in respiratory care and anesthesia.

Table 1. Molecular weight and density derived from Equation (1) of a selection of gases used in respiratory care and anesthesia.

Gas	M	Density 0 °C	Density 20 °C	Density 37 °C
	g/mol	g/m^3	g/m^3	g/m^3
Air	28.96	1292.8	1204.6	1138.5
N_2	28.01	1250.6	1165.2	1101.3
O_2	32.00	1428.5	1331.0	1258.0
N_2O	44.01	1964.8	1830.7	1730.3
He	4.00	178.7	166.5	157.4
CO	28.01	1250.4	1165.1	1101.2
CO_2	44.01	1964.7	1830.6	1730.2
Xe	131.30	5861.5	5461.4	5161.9
He 78% O_2 22%	10.16	453.6	422.7	399.5
He 70% O_2 30%	12.40	553.6	515.8	487.5
He 50% O_2 50%	18.00	803.6	748.7	707.7
Xe 70% O_2 30%	101.51	4531.6	4222.3	3990.7
Xe 35% He 35% O_2 30%	56.96	2542.6	2369.1	2239.1

2.3. Viscosity

Viscosity is associated with a fluid's resistance to flow freely. In the classical example of a gas sheared between two flat plates of surface A separated by a distance y, the coefficient of viscosity, μ (in $\frac{kg}{m.s}$ or $Pa.s$), is defined by the equation:

$$\tau = \frac{F}{A} = \mu \frac{du}{dy} \tag{2}$$

where τ is the shear stress, F is the drag force applied to the plate, and $\frac{du}{dy}$ is the velocity gradient at right angles to the plates. According to the generalized kinetic theory of gas [25], in a diluted regime, the gas viscosity can be approximated by:

$$\mu = \frac{2.68 \times 10^{-6}\sqrt{MT}}{\sigma^2 \Omega_v} \tag{3}$$

where σ is the collision diameter (Å), M is the molecular weight of the gas (g/mol), T is the absolute temperature (K), and Ω_v is a dimensionless parameter that depends on the ratio T/T_ϵ, with T_ϵ being an effective temperature characteristic (see Table 2 for the numerical values):

$$\Omega_v \approx 1.147 \left(\frac{T}{T_\epsilon}\right)^{-0.145} + \left(\frac{T}{T_\epsilon} + 0.5\right)^{-2.0} \tag{4}$$

Table 2. Lennard–Jones parameters [26].

Gas	σ	T_ϵ	M
	Å	K	g/mol
He	2.576	10.2	4
Air	3.617	97	28.97
CO_2	3.996	190	44.01
CO	3.59	110	28.01
O_2	3.433	113	32
N_2	3.667	99.8	28.01
N_2O	3.879	220	44.01
Xe	4.009	234.7	131.3

For a mixture of n gases, Wilke's equation can be used to evaluate the viscosity [27]:

$$\mu_{mix} \approx \sum_{i=1}^{n} \frac{x_i \mu_i}{\sum_{j=1}^{n} x_j \phi_{ij}} \tag{5}$$

where

$$\phi_{ij} = \frac{\left[1 + \left(\mu_i/\mu_j\right)^{0.5}\left(M_j/M_i\right)^{0.25}\right]^2}{\left(8 + 8M_i/M_j\right)^{0.5}} \tag{6}$$

M_i and x_i are the molecular weights and the mole fractions, respectively.
x_i can also be expressed in terms of mass fractions $C_i = \rho_i/\rho$ as follows:

$$x_i = \frac{C_i/M_i}{\sum_{j=1}^{n} C_j/M_j} \tag{7}$$

Table 3 lists the calculated viscosities of helium and several other gases used in respiratory care. The kinematic viscosity, $\nu = \mu/\rho$, is also indicated. It should be noted that helium, as confirmed by experimental data, has a slightly higher viscosity than air, which may be a little counterintuitive. As the viscosity of a nonpolar gas is not due to 'frictional' forces, but rather to the transfer of momentum between adjacent layers of fluid, this result

suggests that the effect of the low molecular weight of helium on the momentum transfer is compensated for by a small collision diameter and thus a large mean free path compared with that of air molecules. Following the kinetic theory of gases, a molecule reaching any layer in a gas had its last collision at a distance from the layer equal to 2/3 of the mean free path on average. If we assume that the velocity gradient $\frac{du}{dy}$ is constant over this distance, the average velocity of helium atoms will vary linearly with this mean free path [28]. Thus, the greater the mean free path, the greater the change in the velocity of the helium atoms crossing the gas layers. This simplified picture of momentum transfer between adjacent gas layers helps to explain the relatively high viscosity of a gas as light as helium.

Table 3. Properties of a selection of gases used in respiratory care (heat capacity values of pure gases retrieved from [29].

Gas	Cp,m	Cp,m (gas)/Cp,m (air)	Cp	μ (20 °C)	μ (37 °C)	k (20 °C)	k (37 °C)	ν (20 °C)	ν (37 °C)
	J/(mol.K)	/	J/(g.K)	μPa.s	μPa.s	mW/(m.K)	mW/(m.K)	mm^2/s	mm^2/s
Air	29.2	1.00	1.008	18.1	18.9	26	27	15.03	16.60
N$_2$	29.1	1.00	1.039	17.5	18.1	25	26	15.02	16.43
O$_2$	29.4	1.01	0.919	20.3	21.1	26	27	15.25	16.77
N$_2$O	38.6	1.32	0.877	14.55	15.4	17	18	7.95	8.90
He	20.8	0.71	5.197	19.5	20.6	153.5	159.6	117.13	130.91
CO	29.1	1.00	1.039	17.4	18.2	26.1	27.3	14.93	16.53
CO$_2$	37.1	1.27	0.843	14.7	15.5	16.2	17.6	8.03	8.96
Xe	20.8	0.71	0.158	22.6	23.8	5.4	5.7	4.14	4.61
He 78% O$_2$ 22%	22.7	0.78	2.233	21.5	22.55	105	109	50.87	56.45
He 70% O$_2$ 30%	23.4	0.80	1.885	21.6	22.6	92	95.1	41.87	46.35
He 50% O$_2$ 50%	25.1	0.86	1.394	21.4	22.3	66	68.2	28.58	31.51
Xe 70% O$_2$ 30%	23.4	0.80	0.230	22.8	23.9	9.6	10.1	5.40	5.99
Xe 35% He 35% O$_2$ 30%	23.4	0.80	0.410	23.7	24.8	34.3	35.7	10.00	11.08

2.4. Thermal Conductivity

Thermal conductivity is the physical property that describes the rate at which heat is conducted. The kinetic theory leads to an expression for the thermal conductivity k in W/(m.K) of a pure dilute gas, which resembles the expression derived for viscosity [25]:

$$k = \frac{0.0833\sqrt{T}}{\sigma^2 \Omega_v \sqrt{M}} \tag{8}$$

For the estimation of the thermal conductivity of dilute mixtures of n gases, Equations (5) and (6) can be used, except that μ_i is replaced in (5) by k_i that is obtained using Equation (8). The calculated conductivities of a selection of gases used in respiratory care are shown in Table 3.

2.5. Heat Capacity at Constant Pressure

The heat capacity describes the amount of heat that must be absorbed by a substance to raise its temperature by 1 °C. For a monoatomic gas, kinetic theory shows that the isobaric molar heat capacity $C_{p,m}$ is:

$$\textit{Monoatomic ideal gas}: C_{p,m} = \frac{5}{2} R \approx 20.786 \text{ J}/(\text{K.mol}) \tag{9}$$

This formula is very accurate for noble gases like helium that indeed have only three degrees of freedom associated with translations in the cartesian plane. Thus, the internal energy of a monoatomic gas is equal to the kinetic energy. A mixture of light and

heavy atoms of noble gases at equilibrium, e.g., He and Xe, will exhibit, on average, the same temperature and therefore the same mean kinetic energy; He atoms simply have a larger mean velocity than Xe atoms. For polyatomic gases, additional degrees of freedom associated with the rotation and vibration of the atoms relative to their center of mass become available as the temperature rises. Thus, polyatomic gases have a larger heat capacity than monoatomic gases, as these additional degrees of freedom, which absorb a part of the heat energy, also contribute to the heat capacity. At ordinary temperatures, a diatomic molecule like O_2 or N_2 has a total of five degrees of freedom, three translational and two rotational; thus, classical theory predicts a molar heat capacity equal to:

$$\text{Diatomic ideal gas}: \ C_{p,m} = \frac{7}{2} R \approx 29.101 \ \text{J}/(\text{K.mol}) \tag{10}$$

In good agreement with experimental data (see Table 3).

Mayer's relation can be used to derive the values of the isochoric molar heat capacity $C_{v,m}$:

$$C_{p,m} - C_{v,m} = R \tag{11}$$

The specific or mass heat capacity of a gas is an intensive property of the substance equal to the heat capacity divided by its molecular weight:

$$C_p = \frac{C_{p, M}}{M} \ \text{J}/(\text{g.K}) \tag{12}$$

The heat capacity of polyatomic gas is usually calculated using empirically derived polynomial fits in temperature (see, e.g., Poling et al. [30]).

For ideal mixtures of n gases, the molar heat capacity at constant pressure is:

$$C_{pmix} = \sum_i x_i C_{pi} \tag{13}$$

where C_{pi} is the molar heat capacity of gas i. The calculated molar and specific heat capacities are shown in Table 3.

2.6. Mass Diffusivity

Diffusion is a mass transfer mechanism that refers to the movement of mass due to molecular exchange. The diffusion of molecules of a given species through itself is called self-diffusion. The binary diffusion coefficient characterizes how molecules of one species placed in the presence of molecules of a second species will mix thanks to molecular collisions to finally reach a homogeneous state of equilibrium. The Chapman–Enskog kinetic theory for dilute gases, in the ideal gas law approximation, gives the following expression for the binary diffusion coefficient D_{12} between species 1 and 2 [25,26]:

$$D_{12} = \frac{0.0018583}{p\sigma_{12}^2\Omega_{D,\,12}} \sqrt{T^3\left(\frac{1}{M_1} + \frac{1}{M_2}\right)} \tag{14}$$

where D_{12} is the binary diffusion coefficient in cm^2/s, M_1 and M_2 are the molecular weights of the two gases in g/mol, $\Omega_{D,\,12}$ is the diffusion collision integral, σ_{12} is the effective collision diameter in Å, T is the absolute temperature in K, and p is the pressure in atm.

The diffusion collision integral can be approximated by [30]:

$$\Omega_{D,\,12} \approx \frac{1.06036}{(T^*)^{0.1561}} + \frac{0.19300}{\exp(0.47635T^*)} + \frac{1.03587}{\exp(1.52996T^*)} + \frac{1.76474}{\exp(3.89411T^*)} \tag{15}$$

where $T^* = T/T_{\epsilon_{12}}$.

The effective temperature and collision diameter, $T_{\epsilon_{12}}$ and σ_{12}, also called the Lennard–Jones potential parameters, are functions of separate molecular properties (see Table 2):

$$T_{\epsilon_{12}} = \sqrt{T_{\epsilon_1} T_{\epsilon_2}} \qquad (16)$$

$$\sigma_{12} = \frac{\sigma_1 + \sigma_2}{2} \qquad (17)$$

The values of the binary diffusion coefficients estimated by these equations typically agree with experimental values to within 5 to 10%.

The diffusion in multicomponent gas mixtures is of particular interest in respiratory care, notably for estimating the diffusion coefficients of carbon dioxide and water vapor through the therapeutic gas. Poling suggests using Blanc's law for a dilute component i diffusing into a homogeneous mixture m:

$$D_{im} = \left(\sum_{j=1,\ j \neq i}^{n} \frac{x_j}{D_{ij}} \right)^{-1} \qquad (18)$$

where $x_j = c_j / c$, c_j is the concentration of i, c is the mixture concentration, and the binary diffusion coefficient D_{ij} of the ij system is assumed to be independent of composition [30].

The binary diffusivities of carbon dioxide and oxygen in a selection of gases at a pressure of 1 atmosphere and temperatures of 20 and 37 °C are presented in Tables 4 and 5, respectively. Binary diffusivities calculated with Fuller's method for additional concentrations of inhaled therapeutic gases are shown in Katz et al. [31].

Table 4. Binary diffusivities at 1 atmosphere.

Gas	D_{i,CO_2} (20 °C)	D_{i,CO_2} (37 °C)
	cm^2/s	cm^2/s
He	0.566	0.622
N$_2$	0.146	0.162
N$_2$O	0.105	0.117
O$_2$	0.146	0.162
Air	0.147	0.163
Xe	0.082	0.091
He 78% O$_2$ 22%	0.346	0.383
He 70% O$_2$ 30%	0.304	0.336
He 50% O$_2$ 50%	0.232	0.257
Xe 70% O$_2$ 30%	0.126	0.140
Xe 35% He 35% O$_2$ 30%	0.182	0.202

Table 5. Binary diffusivities at 1 atmosphere.

Gas	D_{i,O_2} (20 °C)	D_{i,O_2} (37 °C)
	cm^2/s	cm^2/s
He	0.720	0.791
N$_2$	0.197	0.218
N$_2$O	0.147	0.163
Xe	0.119	0.132

3. Flow in a Simplified Lung Airways Model

3.1. Lung Model

Lung airways are divided into the upper respiratory tract, which comprises the nose and nasal cavities, the sinuses, the pharynx, and a part of the larynx, and the lower tract, which is also called the respiratory or airway tree, wherein the branching structure

includes the trachea, bronchi, bronchioles, alveolar ducts, and alveoli. The respiratory tree can be seen, from the trachea to the alveoli, as a succession of circular ducts, each duct being divided into two smaller daughter branches. In humans, there are an average of 23 successive divisions or generations of airways, with internal diameters ranging from around 2 cm in the trachea to a fraction of a millimeter in the most distal airways. The model developed by Weibel in 1962 is one of several lung morphometry models used to describe the generation of branching patterns and the airway geometry in human anatomy [32]. This model was used to analyze the pressure–flow characteristics of the respiratory tree and diffusion phenomena [33]. The Zavala model was also extensively used to analyze steady flow through the central airways. This model consists of 31 main branches terminated by 39 airways (bronchi) of about 3 to 4 mm in inner diameter [34]. Three-dimensional computational fluid dynamics (CFD) models built from computed tomography (CT) [35] or magnetic resonance imaging (MRI) data [36] enable a refined analysis of the airflow through the complex geometry of the airways composed of 2^{23} ducts of various shapes and bifurcations.

3.2. Flow through the Lung Airways

The incompressible steady gas flow through the lung model can be modeled in terms of head losses:

$$\Delta h_{tot} = \sum h_f + \sum h_m \tag{19}$$

where Δh_{tot} is the total head loss, h_f is the Moody-type friction loss, and h_m represents local or minor losses due to any components like the duct entrance or exit, bends, elbows, sudden expansion or contraction, bifurcations, orifices, etc., that induce a change in the fluid velocity [25].

Equation (19) can therefore be rewritten as:

$$\Delta h_{tot} = \sum f \frac{L}{d} \frac{V^2}{2g} + \sum K \frac{V^2}{2g} \tag{20}$$

The friction losses, h_f, can be written as:

$$h_f = f \frac{L}{d} \frac{V^2}{2g} \tag{21}$$

where f is the Darcy friction factor, L is the duct length, d is the duct inner diameter, g is the gravitational acceleration, and V is the average fluid velocity.

The minor losses, h_m, are equal to:

$$h_m = K \frac{V^2}{2g} \tag{22}$$

where the dimensionless loss or resistance coefficient K can be written as:

$$K = \frac{\Delta p}{\frac{1}{2} \rho V^2} \tag{23}$$

where $\Delta p = \rho g h_m$ is the pressure drop induced by the local loss. Many textbooks provide formulae and tables to determine the values of the loss coefficients, K, for various configurations and geometries [25,37]. The specific morphology and constants for the minor loss coefficients of the lung model were calculated by Katz et al. [38].

The friction factor f depends on the duct roughness, its shape, and the Reynolds number, Re_d, defined by:

$$Re_d = \frac{\rho V d}{\mu} \tag{24}$$

The determination of the Reynolds number, which is the ratio of the inertial to the viscous forces within a fluid, is very useful for characterizing the flow regime. Below 2300, the flow in a circular duct is laminar with only minor flow disturbances that quickly vanish. The range of Re_d numbers between 2300 and 4000 is called the transition to turbulence region, as intermittent turbulence occurs. Above 4000, the flow is turbulent with a moderate-to-small Re_d number dependence [37].

In the laminar regime, the friction factor can be easily derived by combining the Poiseuille flow equation in a circular duct (25):

$$\Delta p = \frac{128 \mu L}{\pi d^4} Q \tag{25}$$

where $Q = \frac{\pi d^2 V}{4}$ is the flow rate, and with Equation (21) it can be written as:

$$f = \frac{64}{Re_d} \tag{26}$$

In the laminar regime, the pressure drop varies linearly with the average velocity. For $2300 \leq Re \leq 4000$, the duct flow is unstable as a result of the onset of turbulence and the friction factor is subject to considerable uncertainty.

For transition to moderately turbulent flow, with the Re_d number in the range from 4000 to 10^5, the Blasius approximation can be used:

$$f = 0.316 Re_d^{-1/4} \tag{27}$$

Combining Equations (21) and (26) yields the expression of the pressure drop, Δp, as a function of the flow rate in the turbulent regime:

$$\Delta p = 0.241 L \rho^{3/4} \mu^{1/4} d^{-4.75} Q^{1.75} \tag{28}$$

This approximation allows us to explain the increase in the pressure drop as the 1.75 power of the velocity, which is in good agreement with experimental data (see Figure 1).
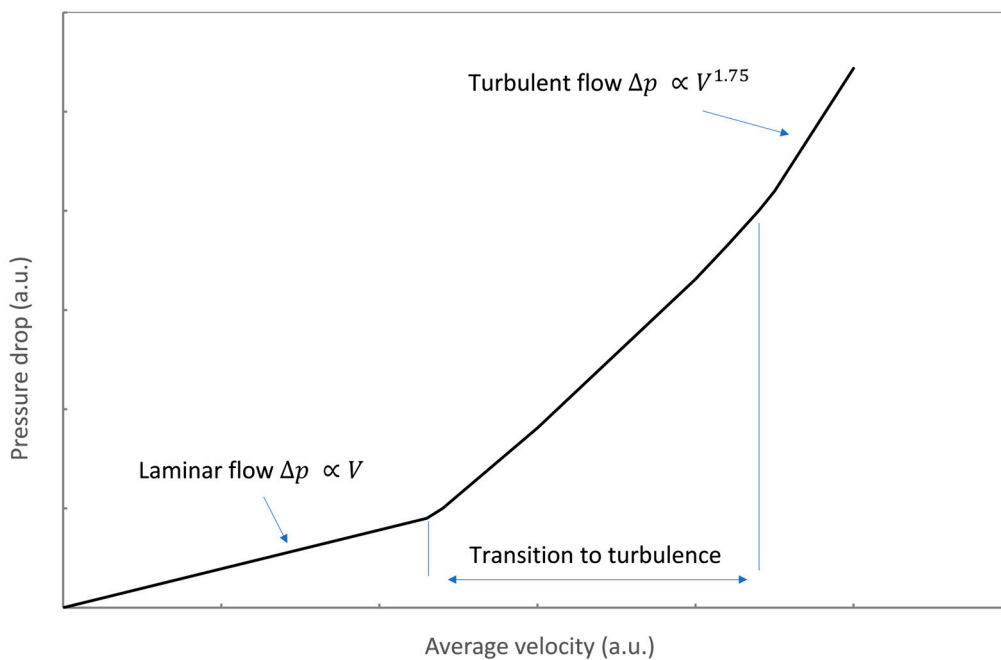

Figure 1. Typical evolution of the pressure drop in a duct as a function of the average velocity during the transition from laminar to turbulent flow.

Figure 1 highlights that laminar flow is more efficient than turbulent flow, as less resistance is observed. Turbulent flow requires additional driving pressure to reach a given flow rate due to higher energy losses.

4. Breathing and Inhaling Mixtures of Helium and Oxygen

4.1. Reduction in the Work of Breathing

The estimations of the Reynolds numbers in the respiratory tract show that the flow is moderately turbulent in the upper airways and becomes laminar after a few generations of airway bifurcations [34,38,39]. As calculated in Section 2, the viscosity of oxygen and helium mixtures is slightly larger than that of air, while its density is lower. Thus, the transition to turbulence for such a gas mixture occurs at a larger average velocity:

$$\frac{V_{transition\ (mix)}}{V_{transition\ (air)}} = \frac{\mu_{mix}}{\rho_{mix}} / \frac{\mu_{air}}{\rho_{air}} = \frac{\nu_{mix}}{\nu_{air}} \tag{29}$$

Table 6 shows the values of this ratio for a selection of gas mixtures at 37 °C. Replacing nitrogen with helium leads to a significant increase in the average velocity at the transition to turbulence by a factor of about 2 to 3. According to Figure 1, the resistance to flow, at a given respiratory rate, will therefore decrease since the linear regime is shifted towards larger flow rates. The presence of xenon, which is notably used in anesthesia, leads to the opposite results, and additional work of breathing (WOB) is required.

Table 6. Kinematic viscosity ratios at 37 °C for a selection of therapeutic gases.

Gas	ν (37 °C)	ν(mix)/ν(Air) (37 °C)
	mm^2/s	
Air	16.60	/
He 78% O$_2$ 22%	56.45	3.40
He 70% O$_2$ 30%	46.35	2.79
He 50% O$_2$ 50%	31.51	1.90
Xe 70% O$_2$ 30%	5.99	0.36
Xe 35% He 35% O$_2$ 30%	11.08	0.67

Reduced turbulence is the explanation most often cited for the advantage of breathing oxygen–helium mixtures [40–49]. In the turbulent regime, the pressure drop is reduced, in agreement with Equation (28), for a gas mixture with a density lower than that of air. The complexity of the respiratory tree and a large number of bifurcations, bends, changes in cross-section, etc., suggest that singular losses may not be negligible, even in the laminar regime. These singular losses, which cause the respiratory gas to accelerate or decelerate, depend on the kinetic energy and thus the density:

$$(\Delta p)_m = \frac{1}{2}\rho V^2 K \tag{30}$$

where $(\Delta p)_m$ is the pressure drop induced by a singular or minor loss. A careful analysis of the impact of these singular losses was carried out by Katz et al. [38]. It was shown that up to generation 10, for a Reynolds number of about 60 with air, significant inertial losses can be observed. This result, which suggests that helium also reduces flow resistance in the laminar regime, is consistent with theory and other research, particularly in the field of passive flow control for medical applications, where minor losses in the laminar regime must be taken into account to obtain the desired constant flow rate [50–55]. The importance of these inertial losses in respiratory mechanics has also been reported in other studies [56–60].

Today, helium–oxygen mixtures are mainly used for patients with obstructions of the upper airways, including the intrathoracic airways and inducible laryngeal obstruction (iLO) [61,62]. Other recognized clinical uses for lower-airway-obstructive diseases

include acute asthma, bronchiolitis, and chronic obstructive pulmonary disease (COPD), particularly for improving exercise tolerance in patients with COPD [48,63,64]. However, there is insufficient evidence to support the use of helium–oxygen mixtures to treat acute exacerbations of COPD in either ventilated or non-ventilated patients [42,48,65]. From a clinical point of view, helium, by diminishing the respiratory frequency and work of breathing, unloads the respiratory muscles, i.e., the diaphragm, the ribcage muscles, and the abdominal muscles. The benefits of breathing helium–oxygen mixtures can be seen after just one hour of treatment [48,62]. It is important to note that helium is not an active drug. This is a "bridge therapy" that mainly relieves the patient's respiratory effort while waiting for the curing of the pathological obstruction using antibiotherapy, bronchodilators, or steroids [48]. Other applications of helium as a diagnostic tool in respiratory care have recently been investigated in several clinical trials. Recent studies have shown that hyperpolarized helium 3 MRI lung scans can help to identify patients at risk of progressing from asthma to fixed airflow obstruction and COPD [66,67].

4.2. Improved Diffusivity

As reported in Table 4, the improved diffusivity of carbon dioxide in mixtures of helium and oxygen, by comparison with air, suggests that such therapeutic gases may improve the elimination of CO_2 and reduce the risk of hypercapnia [68–70]. To explain the observed benefit of breathing helium in terms of reducing the partial pressure of carbon dioxide, $PaCO_2$, there is still a lack of clinical data to determine which is the most relevant parameter between molecular diffusion and the reduction in the work of breathing that notably reduces the production of CO_2 [69,71].

Improved diffusivity is also a factor that may also have, together with the reduction in the flow resistance, a positive impact on the regional deposition of inhaled particles [59,72]. Physical processes that affect the efficiency of particle deposition are discussed by Katz et al. [73]. Three-dimensional imaging has shown deeper and more homogeneous deposition distributions with helium–oxygen mixtures than air, and this result is supported with CFD results. Here again, the results of clinical trials are mixed, and no consensus has been reached despite many positive results [49,59,74–77].

4.3. Thermal Effects

A typical misconception associated with the use of helium in respiratory care is its hypothetic hypothermic effect, probably due to the large value of its specific or mass heat capacity, which is the molar heat capacity divided by the molecular weight of the substance. For a given inspired volume of a helium–oxygen mixture, the small mass of helium compared to that of oxygen balances this large value of the mass heat capacity. As discussed in Section 2, all monoatomic gases indeed have the same molar heat capacity. Thus, the molar heat capacity of a gas mixture that is considered an ideal gas shall be considered here. The gases entering the lungs are heated to 37 °C and saturated by water vapor, with the absolute pressure remaining approximately constant during breathing. The amount of heat transferred to the inspired gases during inspiration is proportional to the number of gas moles and thus the gas volume, the molar heat capacity of the gases, and the difference in temperature between the lung and outside. As reported in Table 3, a gas mixture of oxygen and helium is rather slightly hyperthermic compared to air. Replacing He with another noble gas does not change this trend. During respiration, the large conductivity of helium only contributes to the thermalization rate since the final temperature of 37 °C is fixed. For a patient breathing a helium mixture with a mask, the large thermal conductivity of helium, coupled with convection effects, may generate a cool sensation if the gas is not warmed enough. Also, when the patient is surrounded by helium at a low temperature, the same effect may generate hypothermia via skin heat loss [8,78,79].

5. Conclusions

Helium's properties, particularly its low density and high safety profile, make it an attractive solution for adjunctive therapy in respiratory care, including the exacerbation of asthma, bronchiolitis, ARDS, and COPD. The use of helium–oxygen mixtures was also considered to enhance aerosol delivery to the lung periphery and facilitate weaning from mechanical ventilation [80]. Despite a solid theoretical rationale and promising indications obtained during clinical trials over decades, there is currently no consensus for the use of helium–oxygen mixtures in clinical routines, and the place of helium in respiratory care remains unclear. Conflicting clinical studies may result in a too broad enrolment criterion combined with a limited sample size. Studies have suggested that the location of broncho-restrictions may significantly change the effectiveness of helium in reducing the work of breathing. If the main flow restriction is in the lower bronchioles or distal generations, wherein the flow is non-inertial, helium will not provide significant benefits [81]. Helium probably deserves a large cohort control study that considers, during inclusion or at least during the analysis of the significance of the results, the exact locations of the airway restriction in the respiratory tree. This type of trial would help to confirm the theoretical expectations about the potential benefits of helium as an adjunct therapy in patients with pathological restrictions located in regions of the lungs wherein the flow is inertial ($Re \gg 1$).

Conflicts of Interest: The author is an employee of Debiotech SA and declares no conflict of interest.

References

1. Van Sciver, S.W.; Timmerhaus, K.D.; Clark, A.F. *Helium Cryogenics*; Springer: New York, NY, USA, 2012.
2. Palani, P.K.; Murugan, N. Selection of parameters of pulsed current gas metal arc welding. *J. Mater. Process. Technol.* **2006**, *172*, 1–10.
3. Nagai, H.; Noda, K.; Yamazaki, I.; Mori, T. Status of H-II rocket first stage propulsion system. *J. Propuls. Power* **1992**, *8*, 313–319. [CrossRef]
4. Reich, G. Leak detection with tracer gases; sensitivity and relevant limiting factors. *Vacuum* **1987**, *37*, 691–698. [CrossRef]
5. Beenaker, C.I.M. Evaluation of a microwave-induced plasma in helium at atmospheric pressure as an element-selective detector for gas chromatography. *Spectrochim. Acta Part. B At. Spectrosc.* **1977**, *32*, 173–187. [CrossRef]
6. Häussinger, P.; Glatthaar, R.; Rhode, W.; Kick, H.; Benkmann, C.; Weber, J.; Wunschel, H.J.; Stenke, V.; Leicht, E.; Stenger, H. Noble gases. In *Ullmann's Encyclopedia of Industrial Chemistry*; Verlag Chemie: Hoboken, NJ, USA, 2000.
7. Sayers, R.R.; Yant, W.P. The Value of Helium-Oxygen Atmosphere in Diving and Caisson Operations. *Anesth. Analg.* **1926**, *5*, 127–138. [CrossRef]
8. Berganza, C.J.; Zhang, J.H. The role of helium gas in medicine. *Med. Gas Res.* **2013**, *3*, 18–24. [CrossRef]
9. Postek, M.T.; Vladar, A.E.; Kramar, J.; Stern, L.A.; Notte, J.; McVey, S. Helium ion microscopy: A new technique for semiconductor metrology and nanotechnology. In *AIP Conference Proceedings*; American Institute of Physics: New York, NY, USA, 2007; Volume 931, pp. 161–167.
10. Bouchiat, M.A.; Carver, T.R.; Varnum, C.M. Nuclear polarization in He^3 gas induced by optical pumping and dipolar exchange. *Phys. Rev. Lett.* **1960**, *5*, 373–375. [CrossRef]
11. Yang, X.; Cheng, Y.; Cheng, N.; Gong, J.; Bai, L.; Zhao, L.; Deng, Y. Gases for establishing pneumoperitoneum during laparoscopic abdominal surgery. *Cochrane Database Syst. Rev.* **2022**, *3*.
12. Oei, G.T.; Weber, N.C.; Hollmann, M.W.; Preckel, B. Cellular effects of helium in different organs. *J. Am. Soc. Anesthesiol.* **2010**, *112*, 1503–1510. [CrossRef]
13. Dickinson, R.; Franks, N.P. Bench-to-bedside review: Molecular pharmacology and clinical use of inert gases in anesthesia and neuroprotection. *Crit. Care* **2010**, *14*, 229. [CrossRef]
14. Barach, A.L.; Eckman, M. The Use of Helium as a New Therapeutic Gas. *Curr. Res. Anesth. Analg.* **1935**, *14*, 210–215. [CrossRef]
15. Aver, E.; Olive, K.A.; Skillman, E.D. A new approach to systematic uncertainties and self-consistency in helium abundance determinations. *J. Cosmol. Astropart. Phys.* **2010**, *2010*, 003. [CrossRef]
16. Cooke, R.J.; Fumagalli, M. Measurement of the primordial helium abundance from the intergalactic medium. *Nat. Astron.* **2018**, *2*, 957–961. [CrossRef]
17. Alpher, R.A.; Bethe, H.; Gamow, G. The origin of chemical elements. *Phys. Rev.* **1948**, *73*, 803–804. [CrossRef]

18.   Hoyle, F.; Tayler, R.J. The mystery of the cosmic helium abundance. *Nature* **1964**, *203*, 1108–1110. [CrossRef]
19.   Langer, N.; Henkel, C. The synthesis of helium and CNO isotopes in massive stars. *Space Sci. Rev.* **1995**, *74*, 343–353. [CrossRef]
20.   Lie-Svendsen, Ø.; Rees, M.H. Helium escape from the terrestrial atmosphere: The ion outflow mechanism. *J. Geophys. Res. Space Phys.* **1996**, *101*, 2435–2443. [CrossRef]
21.   Oliver, B.M.; Bradley, J.G.; Farrar, H., IV. Helium concentration in the Earth's lower atmosphere. *Geochim. Cosmochim. Acta* **1984**, *48*, 1759–1767. [CrossRef]
22.   Lockyer, W. Helium: Its Discovery and Applications. *Nature* **1920**, *105*, 360–363. [CrossRef]
23.   Wheeler, M. *Helium: The Disappearing Element*; Springer: Berlin/Heidelberg, Germany, 2015.
24.   Kramer, D. Helium is again in short supply. *Phys. Today* **2022**. [CrossRef]
25.   White, F.M. *Viscous Fluid Flow*, 2nd ed.; McGraw-Hill: New York, NY, USA, 1991.
26.   Bird, B.; Steward, W.; Lightfoot, E. *Transport Phenomena*, 2nd ed.; John Wiley & Sons: New York, NY, USA, 2002.
27.   Wilke, C.R. A viscosity equation for gas mixtures. *J. Chem. Phys.* **1950**, *18*, 517–519. [CrossRef]
28.   Sears, F.W.; Salinger, G.L. *Thermodynamics, Kinetic Theory, and Statistical Thermodynamics*, 3rd ed.; Addison-Wesley: Reading, MA, USA, 1975.
29.   Lide, D.R. (Ed.) *CRC Handbook of Chemistry and Physics*, 78th ed.; CRC Press: Boca Raton, FL, USA, 1997.
30.   Poling, B.E.; Prausnitz, J.M.; O'connell, J.P. *Properties of Gases and Liquids*, 5th ed.; McGraw-Hill Education: New York, NY, USA, 2001.
31.   Katz, I.; Caillibotte, G.; Martin, A.R.; Arpentinier, P. Property value estimation for inhaled therapeutic binary gas mixtures: He, Xe, N_2O, and N_2 with O_2. *Med. Gas Res.* **2011**, *1*, 28. [CrossRef] [PubMed]
32.   Weibel, E.R.; Gomez, D.M. Architecture of the human lung: Use of quantitative methods establishes fundamental relations between size and number of lung structures. *Science* **1962**, *137*, 577–585. [CrossRef] [PubMed]
33.   Weibel, E.R.; Sapoval, B.; Filoche, M. Design of peripheral airways for efficient gas exchange. *Respir. Physiol. Neurobiol.* **2005**, *148*, 3–21. [CrossRef]
34.   Slutsky, A.S.; Berdine, G.G.; Drazen, J.M. Steady flow in a model of human central airways. *J. Appl. Physiol.* **1980**, *49*, 417–423. [CrossRef] [PubMed]
35.   Mihaescu, M.; Gutmark, E.; Murugappan, S.; Elluru, R.; Cohen, A.; Willging, J.P. Modeling flow in a compromised pediatric airway breathing air and heliox. *Laryngoscope* **2008**, *118*, 2205–2211. [CrossRef]
36.   Lewis, T.A.; Tzeng, Y.S.; McKinstry, E.L.; Tooker, A.C.; Hong, K.; Sun, Y.; Mansour, J.; Handler, Z.; Albert, M.S. Quantification of airway diameters and 3D airway tree rendering from dynamic hyperpolarized 3He magnetic resonance imaging. *Magn. Reson. Med. Off. J. Int. Soc. Magn. Reson. Med.* **2005**, *53*, 474–478. [CrossRef]
37.   Chappel, E. (Ed.) *Drug Delivery Devices and Therapeutic Systems*; Academic Press: New York, NY, USA, 2020. [CrossRef]
38.   Katz, I.M.; Martin, A.R.; Muller, P.A.; Terzibachi, K.; Feng, C.H.; Caillibotte, G.; Sandeau, J.; Texereau, J. The ventilation distribution of helium–oxygen mixtures and the role of inertial losses in the presence of heterogeneous airway obstructions. *J. Biomech.* **2011**, *44*, 1137–1143. [CrossRef]
39.   Wang, C.S. *Inhaled Particles*; Elsevier: Amsterdam, The Netherlands, 2005.
40.   Gluck, E.H.; Onorato, D.J.; Castriotta, R. Helium-oxygen mixtures in intubated patients with status asthmaticus and respiratory acidosis. *Chest* **1990**, *98*, 693–698. [CrossRef]
41.   Papamoschou, D. Theoretical validation of the respiratory benefits of helium-oxygen mixtures. *Respir. Physiol.* **1995**, *99*, 183–190. [CrossRef]
42.   Chevrolet, J.C. Helium oxygen mixtures in the intensive care unit. *Crit. Care* **2001**, *5*, 179–181. [CrossRef] [PubMed]
43.   Jolliet, P.; Tassaux, D. Helium-oxygen ventilation. *Respir. Care Clin. N. Am.* **2002**, *8*, 295–307. [CrossRef] [PubMed]
44.   Brighenti, C.; Barbini, P.; Gnudi, G.; Cevenini, G.; Pecchiari, M.; D'Angelo, E. Helium–oxygen ventilation in the presence of expiratory flow-limitation: A model study. *Respir. Physiol. Neurobiol.* **2007**, *157*, 326–334. [CrossRef]
45.   O'Donnell, D.E.; Banzett, R.B.; Carrieri-Kohlman, V.; Casaburi, R.; Davenport, P.W.; Gandevia, S.C.; Gelb, A.F.; Mahler, D.A.; Webb, K.A. Pathophysiology of dyspnea in chronic obstructive pulmonary disease: A roundtable. *Proc. Am. Thorac. Soc.* **2007**, *4*, 145–168. [CrossRef]
46.   Kim, I.K.; Corcoran, T. Recent developments in heliox therapy for asthma and bronchiolitis. *Clin. Pediatr. Emerg. Med.* **2009**, *10*, 68–74. [CrossRef]
47.   Frazier, M.D.; Cheifetz, I.M. The role of heliox in paediatric respiratory disease. *Paediatr. Respir. Rev.* **2010**, *11*, 46–53. [CrossRef]
48.   Slinger, C.; Slinger, R.; Vyas, A.; Haines, J.; Fowler, S.J. Heliox for inducible laryngeal obstruction (vocal cord dysfunction): A systematic literature review. *Laryngoscope Investig. Otolaryngol.* **2019**, *4*, 255–258. [CrossRef]
49.   Lew, A.; Morrison, J.M.; Amankwah, E.; Sochet, A.A. Heliox for pediatric critical asthma: A multicenter, retrospective, registry-based descriptive study. *J. Intensive Care Med.* **2022**, *37*, 776–783. [CrossRef]
50.   Chappel, E. Design and characterization of a passive flow control valve dedicated to the hydrocephalus treatment. *Cogent Eng.* **2016**, *3*, 1247612. [CrossRef]
51.   Cornaggia, L.; Conti, L.; Hannebelle, M.; Gamper, S.; Dumont-Fillon, D.; Van Lintel, H.; Renaud, P.; Chappel, E. Passive flow control valve for protein delivery. *Cogent Eng.* **2017**, *4*, 1413923. [CrossRef]

52. Dumont-Fillon, D.; Lamaison, D.; Chappel, E. Design and Characterization of 3-Stack MEMS-Based Passive Flow Regulators for Implantable and Ambulatory Infusion Pumps. *J. Microelectromech. Syst.* **2020**, *29*, 170–181. [CrossRef]
53. Tachatos, N.; Chappel, E.; Dumont-Fillon, D.; Meboldt, M.; Daners, M.S. Posture related in-vitro characterization of a flow regulated MEMS CSF valve. *Biomed. Microdevices* **2020**, *22*, 21. [CrossRef]
54. Chappel, E. A review of Passive Constant Flow Regulators for microfluidic applications. *Appl. Sci.* **2020**, *10*, 8858. [CrossRef]
55. Chappel, E. Design and Characterization of an Adjustable Passive Flow Regulator and Application to External CSF Drainage. *Micromachines* **2023**, *14*, 675. [CrossRef] [PubMed]
56. Pedley, T.J.; Schroter, R.C.; Sudlow, M.F. The prediction of pressure drop and variation of resistance within the human bronchial airways. *Respir. Physiol.* **1970**, *9*, 387–405. [CrossRef] [PubMed]
57. Despas, P.J.; Leroux, M.; Macklem, P.T. Site of airway obstruction in asthma as determined by measuring maximal expiratory flow breathing air and a helium-oxygen mixture. *J. Clin. Investig.* **1972**, *51*, 3235–3243. [CrossRef]
58. Jaber, S.; Fodil, R.; Carlucci, A.; Boussarsar, M.; Pigeot, J.; Lemaire, F.; Harf, A.; Lofaso, F.; Isabey, D.; Brochard, L. Noninvasive ventilation with helium–oxygen in acute exacerbations of chronic obstructive pulmonary disease. *Am. J. Respir. Crit. Care Med.* **2000**, *161*, 1191–1200. [CrossRef]
59. Corcoran, T.E.; Gamard, S. Development of aerosol drug delivery with helium oxygen gas mixtures. *J. Aerosol Med.* **2004**, *17*, 299–309. [CrossRef]
60. Martin, A.R.; Katz, I.M.; Jenöfi, K.; Caillibotte, G.; Brochard, L.; Texereau, J. Bench experiments comparing simulated inspiratory effort when breathing helium-oxygen mixtures to that during positive pressure support with air. *BMC Pulm. Med.* **2012**, *12*, 62. [CrossRef]
61. Reuben, A.D.; Harris, A.R. Heliox for asthma in the emergency department: A review of the literature. *Emerg. Med. J.* **2004**, *21*, 131–135. [CrossRef]
62. Laude, E.A.; Duffy, N.C.; Baveystock, C.; Dougill, B.; Campbell, M.J.; Lawson, R.; Jones, P.W.; Calverley, P.M. The effect of helium and oxygen on exercise performance in chronic obstructive pulmonary disease: A randomized crossover trial. *Am. J. Respir. Crit. Care Med.* **2006**, *173*, 865–870. [CrossRef] [PubMed]
63. Hashemian, S.M.; Fallahian, F. The use of heliox in critical care. *Int. J. Crit. Illn. Inj. Sci.* **2014**, *4*, 138–142. [CrossRef] [PubMed]
64. Liet, J.M.; Ducruet, T.; Gupta, V.; Cambonie, G. Heliox inhalation therapy for bronchiolitis in infants. *Cochrane Database Syst. Rev.* **2015**, *9*. [CrossRef]
65. Rodrigo, G.J.; Pollack, C.V.; Rodrigo, C.; Rowe, B.H.; Walters, E.H.; Cochrane Airways Group. Heliox for treatment of exacerbations of chronic obstructive pulmonary disease. *Cochrane Database Syst. Rev.* **1996**, *2010*, CD003571. [CrossRef]
66. Eddy, R.L.; Svenningsen, S.; Licskai, C.; McCormack, D.G.; Parraga, G. Hyperpolarized helium 3 MRI in mild-to-moderate asthma: Prediction of postbronchodilator reversibility. *Radiology* **2019**, *293*, 212–220. [CrossRef] [PubMed]
67. Mummy, D.G.; Carey, K.J.; Evans, M.D.; Denlinger, L.C.; Schiebler, M.L.; Sorkness, R.L.; Jarjour, N.N.; Fain, S.B. Ventilation defects on hyperpolarized helium-3 MRI in asthma are predictive of 2-year exacerbation frequency. *J. Allergy Clin. Immunol.* **2020**, *146*, 831–839. [CrossRef]
68. Debiński, W.; Kłossowski, M.; Gembicka, D. Effect of breathing of a helium-oxygen mixture on the adaptation of the organism to exercise. *Acta Physiol. Pol.* **1984**, *35*, 285–292.
69. Beurskens, C.J.; Brevoord, D.; Lagrand, W.K.; van den Bergh, W.M.; Vroom, M.B.; Preckel, B.; Horn, J.; Juffermans, N.P. Heliox improves carbon dioxide removal during lung protective mechanical ventilation. *Crit. Care Res. Pract.* **2014**, *2014*, 954814. [CrossRef]
70. Ho, A.M.H.; Dion, P.W.; Karmakar, M.K.; Chung, D.C.; Tay, B.A. Use of heliox in critical upper airway obstruction: Physical and physiologic considerations in choosing the optimal helium: Oxygen mix. *Resuscitation* **2002**, *52*, 297–300. [CrossRef]
71. Diehl, J.L.; Peigne, V.; Guérot, E.; Faisy, C.; Lecourt, L.; Mercat, A. Helium in the adult critical care setting. *Ann. Intensive Care* **2011**, *1*, 24. [CrossRef]
72. Abroug, F.; Ouanes-Besbes, L.; Hammouda, Z.; Benabidallah, S.; Dachraoui, F.; Ouanes, I.; Jolliet, P. Noninvasive ventilation with helium–oxygen mixture in hypercapnic COPD exacerbation: Aggregate meta-analysis of randomized controlled trials. *Ann. Intensive Care* **2017**, *7*, 59.
73. Katz, I.; Pichelin, M.; Montesantos, S.; Majoral, C.; Martin, A.; Conway, J.; Fleming, J.; Venegas, J.; Greenblatt, E.; Caillibotte, G. Using helium-oxygen to improve regional deposition of inhaled particles: Mechanical principles. *J. Aerosol Med. Pulm. Drug Deliv.* **2014**, *27*, 71–80. [PubMed]
74. Anderson, M.; Svartengren, M.; Bylin, G.; Philipson, K.; Camner, P. Deposition in asthmatics of particles inhaled in air or in helium-oxygen. *Am. J. Respir. Crit. Care Med.* **1993**, *147*, 524–528. [CrossRef]
75. Kim, I.K.; Saville, A.L.; Sikes, K.L.; Corcoran, T.E. Heliox-driven albuterol nebulization for asthma exacerbations: An overview. *Respir. Care* **2006**, *51*, 613–618. [PubMed]
76. Rose, J.S.; Panacek, E.A.; Miller, P. Prospective randomized trial of heliox-driven continuous nebulizers in the treatment of asthma in the emergency department. *J. Emerg. Med.* **2002**, *22*, 133–137. [CrossRef]
77. Hess, D.R. Aerosol delivery devices in the treatment of asthma. *Respir. Care* **2008**, *53*, 699–725.
78. Carr, J.; Jung, B.; Chanques, G.; Jaber, S. Helium as a therapeutic gas: An old idea needing some new thought. In *New Developments in Mechanical Ventilation: European Respiratory Monograph 55*; ERP: Sheffield, UK, 2012; pp. 124–132.

79. Hess, D.R.; Fink, J.B.; Venkataraman, S.T.; Kim, I.K.; Myers, T.R.; Tano, B.D. The history and physics of heliox. *Respir. Care* **2006**, *51*, 608–612.
80. Venkataraman, S.T. Heliox during mechanical ventilation. *Respir. Care* **2006**, *51*, 632–639. [PubMed]
81. Pozin, N.; Montesantos, S.; Katz, I.; Pichelin, M.; Grandmont, C.; Vignon-Clementel, I. Calculated ventilation and effort distribution as a measure of respiratory disease and Heliox effectiveness. *J. Biomech.* **2017**, *60*, 100–109.